1.0 Introduction

Approximately 19% of the Earth's land area and over 50% of its population are exposed to at least one natural hazard, including earthquakes, landslides, floods, volcanoes, cyclones and drought (Dilley et al. 2005). There is, therefore, great interest in efforts to map risks due to hazards globally. The United Nations defines risk as 'the probability of harmful consequences or expected loss of lives, people injured, property, livelihoods, economic activity disrupted (or environment damaged) resulting from interactions between natural or human induced hazards and vulnerable conditions' (UNDP, 2004). In particular, multi-risk approaches at the global level aim to identify the relative levels of overall risk, highlighting the nations where risk is highest (Carpignano et al. 2009).

State-of-the-art global multiple hazard and risk maps include Munich Re's World Map of Natural Hazards, the United Nations Development Program's (UNDP) Disaster Risk Index (DRI), the World Bank's Hotspots report and the UNU-EHS's World Risk Index (WRI) (Lerner-Lam 2007; UNDP 2004; Peduzzi et al. 2009; Dilley et al. 2005; UNU-EHS 2011). An implicit assumption in all such global risk maps is that the risk sources are independent (Kappes et al. 2012). However, this assumption may be naiive, leading to the neglect of possible interactions. In principle, a complete multi-hazard assessment should not be based solely on the superposition of distinct single hazard maps (Marzocchi et al. 2009). Natural processes are components of systems, and as such are not independent and separated from each other (Kappes et al. 2010b). Natural processes such as hazards are inter-connected, often in pairs or longer chains, whereby one can trigger the other (e.g. coseismic landslides, volcano-induced tsunamis, landslide-induced tsunamis, hurricane-induced flooding, hurricane-induced landslides, earthquake-induced tsunamis).

Hazards acting in the natural system should not be seen as just the sum of a set of individual components, but instead as a net of interacting parts which, therefore, need to be examined using a more complex modelling approach (Kappes et al. 2010b; Greiving 2006; Marzocchi et al. 2009). Kappes et al. (2012) suggested that since there are only a few studies dealing with multi-hazard interactions, "experience with associated problems is rare and standard approaches are not available". Thus, the area of cascading natural hazards should be given greater attention by researchers.

1.1 Cascading Hazards

The term 'cascading hazards' is used to describe the phenomenon whereby one hazard triggers another (Figure 1). Kappes et al. (2012) define the cascading hazard phenomenon as 'the triggering of one hazard by another, eventually leading to subsequent hazard events'. This phenomenon is also referred to as the 'avalanche' or 'domino' effect or a catastrophe 'chain' (Helbing and Kuhnert 2003).

Shi (2005) divides 'disaster chains' into two separate types. Simultaneous chains occur when multiple hazards cluster at the same time and place, and cause several disasters concurrently (Shi 2005). Serial chains or synergistic events are a succession of disaster events caused by a single hazard with the resultant disasters occurring in turn (Shi 2005; Marzocchi et al. 2009). Catastrophes are often typified by cascading failures disseminating in the system due to the causal dependencies between system constituents (Buzna et al. 2007). In such a case, one strong initial event can trigger a failure avalanche, spreading in a cascade-like manner within a network, with large consequential impacts (Buzna et al. 2006).

The amplification effect of hazard chains, whereby the overall hazard and risk of causally linked processes is amplified in comparison to the aggregation of presumed independent hazards, is an important aspect of cascading hazards (Kappes et al. 2010b; Kappes et al. 2012; Marzocchi et al. 2009). The amplification effect can either be due to chaining (whereby one hazard triggers and increases the effect of the next hazard) or a consequence of the spatial and temporal coincidence of both (Kappes et al. 2010b).

A difficulty in multi-hazard analysis arises due to the comparability of hazards as their characteristics are different (Carpignano et al. 2009; Marzocchi et al. 2009). For example, earthquakes are typically measured on the moment magnitude scale. Landslides are recorded by the area affected or the number of landslides in one event. Flooding is measured by, for example, the depth of water or area inundated. This makes the comparison of the severity of hazards and their interactions difficult. It is easier to compare earthquake events, for example, but more difficult to compare an earthquake event with a flood event as they vary spatially, temporally and in their effects and associated vulnerability. Classification and index schemes can help to overcome this problem, but remain applicable to the one purpose they are designed for and as such cannot be applied elsewhere (Kappes et al. 2012). A way to overcome this problem is by comparing the consequences of hazards such as loss of life,

injury, damage etc. (Kappes et al. 2012; Marzocchi et al. 2009). In this paper, the number of fatalities was used to compare the severity of earthquakes, coseismic landslides and earthquake-and-landslide events.

1.2 Coseismic Landslides

Coseismic landslides refer to topographic slope failure as a result of earthquakes because of the addition of gravitational and seismic accelerations causing short lived stressed in excess of the combined cohesive and frictional strength of the underlying rock and soils (Meunier et al. 2007). Rodriguez et al. (1999) argued that landslides are potentially the most destructive of the secondary geotechnical hazards as a result of earthquakes. Horizontal ground acceleration from seismic shaking exerts additional transient shear stresses and increases to ambient pore water pressures through cyclic gravitational loading, negatively affecting slope stability (Sidle and Ochiai 2006, in Korup 2010).

Keefer (1984) compiled a database of 40 historical earthquakes and their associated landslides from literature and field studies, chosen to sample a variety of climatic, geological and seismic settings of the Earth's major seismic regions. The database of 40 coseismic landslides showed that landslides were responsible for highly variable, but often significant numbers and proportions of casualties and high levels of economic damage (Keefer 2002). Landslides triggered by the M_w7.8 Kansu, China earthquake in 1920 killed 240,000 people; the 1970 Peru earthquake induced a landslide killing 18,000 people (Keefer 2002).

Fatal coseismic landslides often occur in areas of high topographic relief such as the Himalayas, Andes and Alps (Marano et al. 2010). This is consistent with other studies, which have shown that the coseismic spatial distribution is not random, but is a function of distance to the epicentre, slope gradient, slope position and rock type (Keefer 2002; Meunier et al. 2007, both in Korup 2010).

Marano et al. (2010) examined secondary hazards due to earthquakes from the Prompt Assessment of Global Earthquakes for Response Catalog (PAGER-CAT) database of 18,807 earthquakes from 1968 to 2008. PAGER-CAT is a composite earthquake catalogue from published or online databases and reports; eight global earthquake catalogues are included in the database (Allen et al. 2009). The United States Geological Survey's (USGS) Preliminary Determination of Epicenters (PDE) dataset constitutes the main source of earthquake information. PAGER-CAT incorporates events with PDE's preferred magnitude M5.5 or greater and/or any events causing one or more fatalities or injuries (Allen et al.2009). Events from non-tectonic sources (e.g. mining) were excluded from PAGER-CAT (Allen et al. 2009). The PDE is the primary source of information on casualties due to secondary hazards providing a breakdown of casualty types when possible. Marano et al. (2010) found that of the 749 earthquakes in the PAGER-CAT database that caused at least one fatality, 276 triggered at least one landslide, and of these, 43 were reported to have caused one or more deaths due to landslides (Marano et al. 2010). Due to the undifferentiated cause of deaths for some events, it is likely that there are more events for which deaths could be attributed to secondary hazards (Marano et al. 2010). Post-earthquake reconnaissance work is not always carried out, so often the cause of death remains ambiguous, and is often attributed to the initial triggering event (Marano et al. 2010). The 2004 Sumatra tsunami event contributed 227,000 fatalities of the total 238,385 fatalities as a result of all tsunamis during the time period. Marano et al. (2010) considered this an atypical event, which does not represent the non-shaking fatality distribution of events during the timeline. After the removal of deaths attributed to the 2004 Sumatra event, landslides were found to be the cause for 71.1% of all non-shaking deaths due to earthquakes, with tsunamis following second at 11.5% (Marano et al. 2010).

Kappes et al.'s (2012) review of multi-hazard risk stated that "hazard relations and interactions may have unexpected effects and pose threats that are not captured by means of separate single-hazard analyses". It is implicit throughout the literature that cascading hazards result in losses greater than the sum of the independent hazards (Helbing and Kuhnert 2003; Kappes et al. 2010b; Marzocchi et al. 2009). However, there have been no studies to date published in the literature to quantify or substantiate this claim.

This paper used fatality models based on regression analysis to determine which covariates significantly affect the number of fatalities during an earthquake. It is presumed in the literature that cascading events lead to an amplification of losses. The significance of a triggered event on fatalities is, therefore, of particular interest.

2.0 Data

A dataset of 248 global historical earthquakes from 1980 to 2000 where one or more fatalities was incurred was used to represent earthquake events. This dataset reports the number of fatalities along with the earthquake epicentre and moment magnitude. The dataset was compiled from the USGS earthquake database information

and the Emergency Events Database (EM-DAT) fatality data from the Centre for Research on the Epidemiology of Disasters (CRED). Seventy six historical earthquake events were selected randomly and used to assess the accuracy of the earthquake fatality model at a later stage. The remaining 172 global historical earthquakes were used to model earthquake fatalities.

Rodriguez et al.'s (1999) coseismic landslide dataset of 36 coseismic landslides from 1980 to 1997 was used to represent landslide events triggered by earthquakes. The landslides are described as earthquake or seismically induced, and are therefore inferred to be caused directly be seismic shaking rather than by structural failure or geomorphic change. All references to 'earthquake-and-landslides' refer to an event when an earthquake has occurred and has triggered a coseismic landslide during that event. The number of fatalities recorded and referred to in the paper is the total fatalities recorded resulting from the earthquake *and* the landslide event combined. Rodriguez et al.'s (1999) coseismic landslide database was compiled from major seismological and geotechnical journals, symposia and conferences. The dataset contains information on the date, moment magnitude, focal depth, maximum intensity, area affected and number of landslides for each event. This was combined with the PAGER-CAT database to create a database with longitude and latitude of the epicentre of the triggering earthquake and the total number of recorded fatalities. The data were cleaned to remove events causing no fatalities, leaving a dataset which included 18 earthquake-and-landslides.

Information on other factors which may affect the number of fatalities due to earthquakes or earthquake-and-landslides was compiled from various sources (Table 1) and projected into a GIS environment as a set of global maps. The covariates were chosen based on several factors including (i) typical covariates found in the literature for this type of model, (ii) expectations based on the underlying processes and (iii) availability of datasets.

Global gridded population data were used to estimate the number of people living in the area affected by each earthquake (Table 1). Population estimates are provided for 1990, 1995 and 2000 and projected (in 2004, when GPWv3 was released) to 2005 and 2010. If global gridded population data were not available for the year of an earthquake, the population was estimated for the given year by weighted interpolation in time based on temporally neighbouring data. The population data were used to estimate the population exposed to shaking; the method of estimation is explained in more detail in the next section.

Gross Domestic Product (GDP) global grids for 1990 and 2025 were created using the country-level GDP for 1990 and 2025, and projections were downscaled based on the Special Report on Emission Scenarios (SRES) B2 scenario 1990-2100 dataset and Columbia University Centre for International Earth Science Information Networks's (CIESIN) Gridded Population of the World, Version 2 (GPWv2) as a base map (Table 1) (Yetman et al. 2004).

Slope estimates, measured in percentage, were derived from a combination of global SRTM30+ and ETOPO DEM data at 1 arc minute resolution (Table 1). Building strength data were sourced from the USGS Prompt Assessment of Global Earthquakes for Response (PAGER) project on a country-by-country basis (Table 1). The PAGER project divides building strength into five categories, from 1 (strongest) to 5 (weakest).

Access is a measure of travel time in minutes to the nearest major city with population over 50,000 in the year 2000 (Table 1) (Nelson 2008). Accessibility was computed using a cost-distance algorithm which calculates the 'cost' of travelling between two positions on a raster grid (Nelson 2008). Each cell is assigned a value representing the cost required to travel across them; this raster grid is often labeled a 'friction-surface'. The friction-surface contains information on transport network (road, railway, river and shipping lanes), environmental (land cover and slope), and political factors (national boundaries and border crossing) that affect travel times between locations (Nelson 2008).

Poverty was defined as the percentage of population living below the international poverty line at $1.25 (in purchasing power parity in 2000) per day (Table 1). Data were based on primary household survey data obtained from government statistical agencies and the World Bank country departments. The source data from the UNDP were inconsistently recorded. Therefore, if data were missing, the poverty value was estimated using weighted interpolation in time based on temporally neighbouring data.

Health was defined as a measure of public health expenditure as a percentage of GDP in 2000 (Table 1). Public health expenditure consists of current and capital spending from government budgets, external borrowings and grants, and social health insurance funds. Health expenditure data were downloaded at country-level.

The required information for each covariate was extracted from the global covariate maps within a GIS environment using the longitude and latitude of the earthquake epicentre for each earthquake and earthquake-and-landslide event. For each epicentre location, the corresponding cell or country data were extracted and assigned to the event as a proxy for determining other factors which could affect the number of fatalities.

3.0 Estimation of Exposed Population

A key independent variable affecting the number of fatalities is the population potentially affected. The number of fatalities from an earthquake should be related to the number of people exposed to the shaking caused by the earthquake. If the epicentre of the earthquake is closer to highly dense populations, more people will be exposed and a higher number of fatalities is expected. If the epicentre of the earthquake is far from dense populations, less people will be exposed and a small number of fatalities is expected.

USGS ShakeMaps were used to calculate the area affected by different levels of shaking (3.9, 9.2, 18 and 34 pga) using 28 events between 2004 and 2009 ranging from 5.6 to 8.6moment magnitude. Data were not available before this date except for the United States of America. The 28 events were selected from 78 earthquake events recorded in the PAGER-CAT database with one or more fatalities between 2004 and 2009. The selection from the 78 events was based on the availability of ShakeMaps for download from the USGS ShakeMap Archive.

The thresholds for the levels of shaking were taken from the USGS ShakeMap scale for moderate, strong, very strong and severe perceived shaking (Table 2). For each event, the peak ground acceleration (pga) point data recorded by seismometers were projected into a GIS environment and converted into the raster data format. The area affected by the different thresholds of shaking was then estimated for each event (Figure 2). A best fit model was developed from the empirical data relating earthquake moment magnitude to area affected (measured in degrees) and their 95% confidence intervals for each of the different levels of shaking (Figure 3). Four exponential models were fitted to the empirical data:

$$A_{3.9} = 0.0042e^{1.0992\times M} \quad \text{Equation 1}$$
$$A_{9.2} = (1 \times 10^{-5})e^{1.7106\times M} \quad \text{Equation 2}$$
$$A_{18} = (6 \times 10^{-8})e^{2.2792\times M} \quad \text{Equation 3}$$
$$A_{34} = (3 \times 10^{-8})e^{2.1127\times M} \quad \text{Equation 4}$$

Where,
$A_{3.9}$ = area affected by ≥3.9 pga shaking,
$A_{9.2}$ = area affected by ≥9.2 pga shaking,
A_{18} = area affected by ≥18 pga shaking,
A_{34} = area affected by ≥34 pga shaking, and
M = earthquake magnitude.

Table 3 shows the upper and lower 95% confidence intervals for the fitted models shown in Equations 1-4. The root mean square errors between model predictions and the estimated observed area affected were 10.29 for $A_{3.9}$, 25704.24 for $A_{9.2}$, 1.97 for A_{18} and 0.67 for A_{34}. The area affected was then calculated as a transform of the recorded earthquake magnitude for each historical earthquake event from the combined USGS and EM-DAT dataset. The radius r of each area affected was calculated using:

$$\boldsymbol{r} = \sqrt{\frac{\boldsymbol{A}}{\boldsymbol{\pi}}} \quad \text{Equation 5}$$

Circular buffer zones around each event epicentre were generated based on the estimated radius of the affected area (Figure 4). The number of people living within the area exposed to each level of shaking was estimated by intersecting the circular areas with the global gridded population data for the corresponding year from SEDAC.

4.0 Fatalities

The number of fatalities had a right-skewed distribution with a large number of smaller values and a tail of larger values with lower frequency. Therefore, the number of fatalities was transformed using the log function. Figure 5 shows a plot of number of fatalities against seismic magnitude where earthquakes are separated from earthquake-and-landslides. Figure 5 reveals an increase in the number of fatalities for earthquake-and-landslides compared to earthquake events with no landslides. It is also clear that the relationship between number of fatalities from earthquakes and earthquake magnitude is non-linear such that a log-transform of number of fatalities produces an approximately linear relation.

Although an increase in the number of fatalities was predicted, and this seems to match expectations, the magnitude of the uplift in number of fatalities was not expected: the increase in number of fatalities appears to be by a factor of almost ten (Figure 5). The 95% confidence intervals for each best-fit statistical model are shown in Figure 5, and the corresponding coefficients for the best-fit, upper and lower 95% confidence models can be seen in Table 4.

4.1 Multiple regression analysis

Multiple regression analysis was used to model the relationship between the number of fatalities and several independent covariates using the backward stepwise method. The covariates selected were: exposed population, earthquake magnitude, GDP, slope, poverty, health, access to cities, building strength and whether a landslide was triggered or not. Whether there is a landslide or not as a result of an earthquake was coded as a binary variable, representing presence (1) or absence (0) of landslides.

The significant (at the 95% confidence level) covariates were earthquake magnitude (EQ.M), building strength (BS), population exposed to ≥18 pga (PopExp18) and whether a landslide was triggered or not (LS.NoLS). Table 5 shows the covariates in order of significance with their statistics generated by the R statistical software.

The number of fatalities is highly correlated with the number of people exposed to earthquake shaking above 18 pga. The model shows clearly that the presence of a triggered coseismic landslide due to the initial earthquake significantly increases the number of resultant fatalities. The earthquake magnitude and the strength of the buildings affected by the shaking are also contributing factors to the number of fatalities caused. Weaker building structures are more likely to be damaged or collapse during an earthquake and, thus, result in a greater number of fatalities compared to stronger building structures.

The fitted multivariate regression model was:

$$\log(F_E) = -1.806 + 0.3348M + 0.1841BS + 0.9614LS + 0.0000002123PE_{18} \quad \text{Equation 6}$$

Where F_e is the number of fatalities from an earthquake, M is the earthquake moment magnitude, BS is the building strength, LS is whether a landslide was triggered (1) or not (0) and PE_{18} is the population exposed to ≥18 pga shaking, 95% Confidence Interval [-1.95, 0.47].

4.2 City Fatality Estimates

Fatalities due to earthquakes and earthquake-and-landslides for 68 cities around the world were estimated using the fatality model (Equation 6). The global distribution of earthquake risk and global distribution of landslide risk maps from the Hotspots report were used to create a map of areas at risk of both earthquakes and landslides (Figure 6) (Dilley et al. 2005). 68 cities within this zone were selected and the number of fatalities from an earthquake of varying magnitudes (M_w 4, 5, 6, 7, and 8) was estimated using the model (Equation 6).

Global building strength data for each country from PAGER were used (Table 1); the area exposed to shaking above 18 pga was calculated using Equations 3 and 5 to create a circular buffer around each city epicentre for the different earthquake magnitudes. The number of people living within this area was counted using GPW for the year 2010 to estimate the population exposed to ≥18 pga shaking.

The number of fatalities from earthquakes alone and the increase in fatalities expected from landslides being subsequently triggered were estimated for the 68 cities. These fatality data can be seen in Figure 7. The variation in fatality estimates for each magnitude earthquake (Figure 7) arises due to the differences in the population exposed to shaking for each city and in building strength for each country. A selection of the 68 cities shown in Figure 7 was used to predict fatality values in each city using Equation 6 and the 95% confidence intervals of the model for a M_w8 earthquake. This estimates a range of predicted fatalities for each city calculated from the model's 95% confidence interval (seen in Table 6).

The city fatality estimates represent the number of fatalities predicted given an earthquake at the centre of each city. The model predicts the number of fatalities given an earthquake of a given magnitude occurring at the city centre, and the numbers of fatalities if at least one landslide were to occur as a result of the earthquake. However, the model does not attempt to predict the probability of a landslide occurring given the earthquake.

4.3 Comparison with Observed Fatalities

The 76 historical earthquakes held back from the analysis were compared with model predictions. Building strength and the population exposed to 18 pga shaking were estimated using the methods described previously. Of the 76 earthquakes, eight events resulted in triggered landslides.

The root mean square error for earthquake-only fatality estimates compared to the observed fatalities in the validation dataset is 52 fatalities. Two events stand out as outliers, with the number of observed fatalities higher than predicted by the model. For most of the fatal earthquakes in the sample, the estimated number of deaths is within one order of magnitude of those observed. While in the predictive sense such a large ratio of predicted to observed fatalities does not seem noteworthy, in practice the warning level accompanying such a prediction may be valuable and on target for deciding the appropriate level of response (Jaiswal and Wald 2010).

The empirical model over-predicts fatalities during earthquake events with associated landsliding; the root mean square error for the earthquake-and-landslide events is 3,077 fatalities. This lack of predictive ability of the model is most likely due to the small sample size used for earthquake-and-landslide events. Unfortunately, very little data are available for earthquakes that have triggered landslide events. Until a more comprehensive fatality dataset is collated for landslides triggered by earthquakes, the model's predictive ability will remain limited.

5.0 Discussion

The model indicates the significant covariates affecting fatalities during earthquakes. Earthquake magnitude is a significant variable affecting the number of fatalities as expected; this is supported in the literature as the greater the shaking caused by the earthquake, the greater the damage to buildings and, therefore, the number of fatalities. The strength of the building also affects the number of fatalities; in countries with buildings more resistant to earthquake shaking, fewer fatalities are seen. The adage 'earthquakes don't kill people - buildings do' is applicable here. The number of people exposed to shaking also affects the number of fatalities during an event; the more people exposed to shaking, the more people are at risk of death and more fatalities are experienced. Most interestingly, the triggering of landslides increases the risk of fatalities from the secondary hazard. If this landslide occurs where there is a built-up population, there is an associated increase in fatalities compared to if no landslide had occurred.

The selection of the data for each event was determined by the location of the epicentre. However, many of the covariates used in the fatality model were produced from source data representing a range of spatial resolutions. This variation in resolution may not adequately represent the conditions experienced by the area affected by the earthquake. Although the use of data defined at different spatial resolutions is necessary from a practical viewpoint, it may have implications for modelling as the relative importance of the independent variables may be affected. This should be taken into consideration when interpreting the results.

The method of calculating the area affected by different levels of shaking assumes that the area affected is circular, which provides a reasonable approximation for the purpose of estimating the area affected and the population exposed. However, the area affected is unlikely to be perfectly circular in practice, especially for higher levels of shaking and in areas of high relief. The geology of the area was also not included in the calculation of the area affected by shaking.

Poverty, health expenditure and building strength data were recorded at the country-level. These country-level estimates were used as a proxy for the conditions present at the location of the earthquake epicenter. This assumes that these covariates are uniform within a country. In reality, this is not true. However, data at a finer resolution do not exist globally. Also, GDP per capita data for 1990 and 2025 were also originally estimated at the country level before being down-scaled to 15 arc minute resolution using gridded population datasets.

The geology of the area could have a significant impact on the number of fatalities caused by an earthquake due to liquefaction and amplification effects through certain types of rock and soil, and on whether a landslide is triggered or not. Geology was not included in the multiple regression analysis because a consistent global map with sufficient detail was not available. The geology of the area can affect shaking as a result of earthquakes because of the softness and thickness of the upper layer. Shaking increases in softer rocks, when the sediment above hard rock is thicker, and in soil near the surface.

Several high magnitude earthquake events exist in the dataset that were not recorded as having triggered a landslide. It is not guaranteed that these events did not trigger a subsequent landslide. It is, for example, possible

that the area experiencing the earthquake was of low relief and slope. Alternatively, landslides may have occurred, but were not recorded, possibly because they did not cause any fatalities. Alternatively, it is highly unlikely that any landslides which caused a fatality directly went unrecorded.

The earthquake data were cleaned to remove any events below M_w4.0 shaking by the USGS. This could create bias in the sample as smaller earthquakes for which landslides may not be induced were excluded. Therefore, the model can only be applied to earthquake events above the M_w4.0 threshold. Below this level of shaking, the model has little usefulness; however, empirical evidence given by Keefer (1984) suggests few landslides are caused by earthquakes below M_w4.0.

Uncertainty in the model estimates particularly arise because it is unknown whether the landslides that occurred during these historical events affected any of the population. It is plausible that whilst landslides occurred during the events, they did not affect any human populations. The empirical model does not capture the population exposed to landslides. For this to be captured, the area (and associated exposed population) affected by historical coseismic landslides would have to be collated. Such a dataset does not currently exist and is beyond the scope of this investigation.

The association between landslides and increased fatalities is not necessarily directly causal (i.e., landslides cause fatalities adding to the total number of fatalities). It could arise, for example, because both outcomes (landslides, fatalities) are promoted by some underlying common driver. For example, poorer (and therefore more vulnerable) communities are often located on steeper, less stable slopes (El-Masri and Tipple 1997; Kates and Haarmann 1992). During an earthquake event, they may be more vulnerable to the shaking from earthquakes (e.g., because of poorer infrastructure) and could experience a higher proportion of fatalities while landslides also occur in these areas. Floodplains are often occupied by the wealthier population because of geographical access and proximity to rivers and estuaries as resources and centres of trade (Fleming 2002). This wealthier component of the population is likely to be less vulnerable, but is spatially located in an area where landslides are unlikely to occur. Similarly, landslides could block roads and access routes, hampering rescue efforts following an earthquake. The first 24-48 hours of search and rescue following an earthquake are especially important in saving lives. There is a dramatic drop-off in live finds during the 24-48 hour post-earthquake timeframe, with very few live rescues after 10 days (Macintyre et al. 2006). In earthquake-and-landslide events, the landslide may not necessarily be the direct cause of fatalities, but could exacerbate the number of fatalities by reducing access to those trapped or requiring medical assistance in the immediate aftermath of an earthquake. Therefore, the increase in fatalities associated with earthquake-and-landslide events may be, but is not necessarily, directly causal.

To be able to differentiate between the above possibilities (i.e., landslides cause and increase fatalities; an underlying driver such as high slope promotes landslides and increases vulnerability), and ultimately attribute cause, data at a finer spatial resolution than used here would be required. The spatial distribution of each landslide occurrence would need to be correlated with a topographic map of slope, and poverty indicators per household or neighbourhood. Although measures of these factors were used in this study to explore their statistical relations with fatalities, the spatial scale at which they were analysed prevented diagnosis of these potential causal links. Until within-country data are provided, for example on social vulnerability, it will remain an open question.

The uncertainty in hindcasting the total earthquake fatalities using the empirical model incorporates the variability that comes from (a) the uncertainty in the estimated population exposed, (b) the variability of building strengths within countries, (c) possible errors in the number of recorded deaths in the catalogue, and (d) uncertainty in the recorded factors affecting earthquake fatality data. Despite the limited predictive ability for earthquake-and-landslide fatalities, the model is useful in revealing the significant factors affecting fatalities during earthquakes; particularly that landsliding is associated with an increase in the number of fatalities.

Further research should investigate whether economic losses, number of injured, ratio of injured to fatalities and building damage are greater for cascading hazards compared to single hazards. The signal within the data is very small when looking at global examples and when dealing with natural hazards as they are such complex phenomena, affected by many other factors. If we examine a range of hazard outcomes, the signal could be present in other consequences, which would strengthen the overall signal if the numbers involved are greater, or if the multiple outcomes can be analysed simultaneously. For example, whereas people can move their location, affecting fatality rates through evacuation and being outside or inside during an event, economic assets cannot be moved out of the affected area.

The utility of the available data on earthquake events for investigating cascading hazards is limited as records typically assign losses to the primary hazard event. To be able to determine whether cascading events result in greater losses than the sum of the constituent hazards, the fatalities caused by the coseismic landslide alone need to be separated from those caused by the triggering earthquake. This can be achieved by subtracting earthquake-only loss models from earthquake-and-landslide models. The difference between the models would account for those fatalities as a result of the coseismic landslides. The fatality estimates could be used to create a coseismic landslide model based on landslide magnitude.

6.0 Conclusions

The relationship between number of fatalities and earthquakes alone and earthquake-and-landslides was investigated. Regression analysis suggested that the presence of a triggered landslide significantly increases the number of fatalities caused by an earthquake event compared to if no landslide is triggered, independent of other factors including seismic magnitude, building strength and population affected. The model quantifies, for the first time, the effect of triggered landslides in increasing the number of fatalities. This pattern of increased losses as a result of cascading events has previously been referred to, but has been hitherto unsubstantiated, in the literature. The fitted earthquake fatality model can be used to predict the likely human losses as a result of earthquakes given the availability of earthquake magnitude, building strength and population data. Further research into cascading hazards is necessary, but will ultimately be constrained by data availability. Data collection and recording methods are becoming more detailed with wider coverage suggesting that improvements in terms of data quality to the model presented here will be possible in future.

Acknowledgements

We would like to thank the Centre for Research on the Epidemiology of Disasters and U.S. Geological Survey for the provision of earthquake data.

References

Allen TI, Marano KD, Earle PS, and Wald DJ (2009). PAGER-CAT: A composite earthquake catalog for calibrating global fatality models. *Seism. Res. Lett* 80(1): 57-62.

Bovolo IC, Abele SJ, and Bathurst JC (2009) A distributed framework for multi-risk assessment of natural hazards used to model the effects of forest fire on hydrology and sediment yield. *Computers & Geosciences* 35 (5): 924-945.

Bryant (2005) *Natural Hazards.* 2nd ed., Cambridge University Press, New York.

Buzna L, Peters K, Ammoser H,and Helbing D (2007) Efficient response to cascading disaster spreading. *Physical Review E*: 1-7.

Buzna L, Peters K, and Helbing D (2006) Modelling the dynamics of disaster spreading in network. *Physica A: Statistical Mechanics and its Applications* 363 (1): 132-140.

Carpignano A, Golia E, Di Mauro C, Bouchon S, and Nordvik J-P (2009) A methodological approach for the definition of multi-risk maps at regional level: first application. *Journal of Risk Research* 12 (3): 513-534.

Chen Y, Fan KS, and Chen L (2010) Requirements and Functional Analysis of a Multi-Hazard Disaster-Risk Analysis System Requirements and Functional Analysis. Human and Ecological Risk Assessment: An International Journal 16, 2, 413-428.

CIESIN (2005) Gridded Population of the World, Version 3 (GPWv3), Palisades, NY, CIESIN, Columbia University. http//sedac.ciesin.columbia.edu/gpw/index.jsp. Accessed 1st February 2012.

Dilley M, Chen S, Lerner-Lam A (2005) Natural Disaster Hotspots: A Global Risk Analysis. *The World Bank and Columbia University.*

El-Masri S, and Tipple G (1997) Urbanization, poverty and natural disasters: vulnerability of settlements in developing countries. *Reconstruction after Disasters* 12, 2, 141-158.

Fleming G (2002) Learning to live with rivers – the ICE's report to government. *Civil Engineering* 150, 15-21.

Greiving S (2006) Integrated Risk Assessment of Multi-Hazards: A New Methodology. In *Natural and Technological Hazards and Risks Affecting the Spatial Development of European Regions*, ed. P Schmidt-Thome, Geological Survey of Finland, Special Paper 42, 75-82.

Helbing D, and Kuhnert C (2003) Assessing interaction networks with applications to catastrophe dynamics and disaster management. *Physica A: Statistical Mechanics and its Applications* 328 (3-4): 584-606.

Helbing D, Ammoser H and Kühnert C (2005) Disasters as extreme events and the importance of network interactions for disaster response management in S. Albeverio, V. Jentsch and H. Kantz (Eds.) *The Unimaginable and Unpredictable: Extreme Events in Nature and Society*. Berlin: Springer, pp.319–348.

Hengl T and Reuter HI (2010) Worldgrids – a public repository and a WPS for global environmental layers: Slope Map. http://worldgrids.org/doku.php?id=wiki:slpsrt3. Accessed 9th February 2012.

Jaiswal K and Wald DJ (2005) Creating a Global Building Inventory for Earthquake Loss Assessment and Risk Management: Open-File Report 2008-1160: Appendix VII: PAGER_database_v1.4.xls. http//pubs.usgs.gov/of/2008/1160/downloads/PAGER_database/. Accessed 4th March 2012.

Jaiswal KS and Wald D (2010) An Empirical Model for Global Earthquake Fatality Estimation. *Earthquake Spectra* 26, 4, 1017-1037.

Kappes M, Keiler M, and Glade T (2010a) The Relevance of Multi-Hazard Risk Analyses for Risk Reduction in a Dynamic World. *Proceedings of the 2010 Summer Institute for Advanced Study of Hazard and Risk*.

Kappes M, Keiler M, and Glade T (2010b) From Single- to Multi-Hazard Risk Analyses : a concept addressing emerging challenges. In *Mountain Risks: Bringing Science to Society*, ed.s J-P Malet, T Glade and N Casagli, Proceedings of the 'Mountain Risks' International Conference, Nov 2010.

Kappes M, Keiler M, von Elverfeldt K and Glade T (2012) Challenges of analyzing multi-hazard risk: a review. Natural Hazards 64(2), 1925-1958.

Kates RW, and Haarmann (1992) Where the Poor Live: Are the Assumptions Correct? *Environment* 34, 4, 4-11, 25-28.

Keefer DK (1984) Geological Society of America Bulletin Landslides caused by earthquakes. *Geological Society Of America Bulletin* 95, 4, 406-421.

Keefer DK (2002) Investigating landslides caused by earthquakes – a historical review. *Surveys in Geophysics* 23: 473-510.

Kirschbaum DB, Adler R, Hong Y, Hill S and Lerner-Lam A (2009) A global landslide catalog for hazard applications: method, results, and limitations. *Natural Hazards* 52 (3): 561-575.

Korup O (2010) Earthquake-triggered landslides – spatial patterns and impacts. *COGEAR*, Module 1a – Report.

Lerner-Lam A (2007) Assessing global exposure to natural hazards: Progress and future trends. *Environmental Hazards* 7, 10–19.

Lu GY, Chiu LS, and Wong DW (2007) Vulnerability assessment of rainfall-induced debris flows in Taiwan. *Natural Hazards* 43 (2): 223-244.

Macintyre AG, Barbera JA, and Smith ER (2006) Surviving collapsed structure entrapment after earthquakes: a "time-to rescue" analysis. *Prehospital and Disaster Medicine* 21 (1): 4-19.

Marano KD, Wald DJ, and Allen TI (2010) Global earthquake casualties due to secondary effects: a quantitative analysis for improving rapid loss analyses. *Natural Hazards* 52: 319-328.

Marzocchi W, Mastellone ML, and Di Ruocco A (2009) Principles of multi-risk assessment: Interaction amongst natural and man-induced risks. *European Commission* EU 23615.

Meunier P, Houvis N, and Haines JA (2007) Regional patterns of earthquake-triggered landslides and their relation to ground motion. *Geophysical Research Letters* 34: L20408.

Rodriguez CE, Bommer JJ, and Chandler RJ (1999) Earthquake-induced landslides: 1980-1997. *Soil Dynamics and Earthquake Engineering* 18: 325-346.

Nelson A (2008) Travel time to major cities: A global map of Accessibility. Global Environment Monitoring Unit - Joint Research Centre of the European Commission, Ispra Italy. http://www-tem.jrc.it/accessibility. Accessed 9th March 2012.

Peduzzi P, Dao H, Herold C, and Mouton F (2009) Assessing global exposure and vulnerability towards natural hazards : the Disaster Risk Index. *Earth* 1149-1159.

Shi P (2005) Theory and Practice on Disaster System Research. Paper for the Fifth Annual IIASA-DPRI Forum.

UNDP (2004) Reducing Disaster Risk: A Challenge for Development. UNDP Bureau for Crisis Prevention and Recovery, New York, 146pp.

UNDP (2013) International Human Development Indices: Data. http://hdrstats.undp.org/en/tables/. Accessed 1st March 2012.

UNU-EHS (2011) World Risk Report 2011.

Yetman G, Gaffin SR, and Xing X (2004) Global 15 x 15 Minute Grids of the Downscaled GDP Based on the SRES B2 Scenario, 1990 and 2025. Palisades, NY: NASA Socioeconomic Data and Applications Center (SEDAC). http://sedac.ciesin.columbia.edu/data/set/sdp-downscaled-gdp-grid-b2-1990-2025. Accessed 1st March 2012.

Appendix 1

Table A1. A list of the acronyms used.

Acronym	**Description**
CIESIN	Columbia University Centre for International Earth Science Information Network
CRED	Centre for Research on the Epidemiology of Disasters
DEM	Digital Elevation Model
DRI	Disaster Risk Index
EM-DAT	Emergency Events Database
ETOPO	Earth Topography Digital Dataset
GDP	Gross Domestic Product
GIS	Geographical Information System
GPW	Gridded Population of the World
PAGER	Prompt Assessment of Global Earthquakes for Response
PAGER-CAT	Prompt Assessment of Global Earthquakes for Response Catalog
PDE	Preliminary Determination of Epicentres
pga	Peak ground acceleration
SRES	Special Report on Emission Scenarios
SRTM	Shuttle Radar Topography Mission
UNDP	United Nations Development Program
USGS	United Stated Geological Society
WRI	World Risk Index

Table 1. Description, spatial scale and source of data for the covariates used in multiple regression analysis to determine the factors affecting the number of fatalities during earthquake and earthquake-and-landslide events. Gridded population of the world data were used to estimate the number of people affected by different levels of earthquake shaking.

Factor	**Description**	**Spatial scale**	**Source**
Gridded Population	Gridded Population of the World (version 3) per year 1990-2010.	2.5 arc minutes ~5km at the equator	Columbia University Center for International Earth Science Information Network (CIESIN) and Centro International de Agricultura Tropical (CIAT). (CIESIN 2005)
GDP 1990	Gross Domestic Product in 1990 in millions of US dollars.	15 arc minutes ¼ degree	Columbia University Center for International Earth Science Information Network (CIESIN), (Yetman et al. 2004)
GDP 2025	Gross Domestic Product projected for 2025 in millions of US dollars.	15 arc minutes ¼ degree	Columbia University Center for International Earth Science Information Network (CIESIN), (Yetman et al. 2004)
Slope	Derived from SRTM30+ and ETOPO DEM.	1 arc minute 1/120 degree	Worldgrids.org (Hengl and Reuter 2010)
Poverty	Percentage of population living below $1.25 per day in 2000.	Country	UNDP, World Bank (UNDP 2013)
Health	Health expenditure as a percentage of GDP in 2000.	Country	UNDP, World Bank, World Health Organization National Health Account database (UNDP 2013)
Access	Travel time to major cities.	30 arc seconds	European Commission, World Bank. (Nelson 2008)
Building strength	Building strength in 5 categories, from 1 (strongest) to 5 (weakest).	Country	USGS (Jaiswal and Wald 2008)

Table 2. The USGS ShakeMap scale. The USGS produces serveral ShakeMap types. The peak ground acceleration (pga) data were used to determine levels of shaking for estimated area affected. Peak ground acceleration at each station is contoured in units of percent-g (where g = acceleration due to the force of gravity). Thresholds of ⩾3.9 pga (moderate perceived shaking), ⩾9.2 pga (strong perceived shaking), ⩾18 pga (very strong perceived shaking), and ⩾34 pga (severe perceived shaking) were used to provide shaking levels for calculating exposed population to earthquake shaking.

PERCEIVED SHAKING	Not felt	Weak	Light	Moderate	Strong	Very strong	Severe	Violent	Extreme
POTENTIAL DAMAGE	None	None	None	Very light	Light	Moderate	Moderate/ heavy	Heavy	Very heavy
PEAK ACCELERATION (%g)	< .17	.17-1.4	1.4-3.9	3.9-9.2	9.2-18	18-34	34-65	65-124	>124
PEAK VELOCITY (cm/s)	<0.1	0.1-1.1	1.1-3.4	3.4-8.1	8.1-16	16-31	31-60	60-116	>116
INSTRUMENTAL INTENSITY	I	II-III	IV	V	VI	VII	VIII	IX	X+

Table 3. A table of estimated coefficients for Area Affected models seen in Equations 1-4. The upper and lower 95% confidence intervals for each fitted model is shown. This data is shown plotted in Figure 3.

Model	Covariate	Estimated coefficient	95% Confidence Interval	
			Lower limit	Upper limit
$\mathbf{A_{3.9}}$	Intercept	0.0042	0.0056	0.0032
	Earthquake Magnitude	1.0992	1.0075	1.1909
$\mathbf{A_{9.2}}$	Intercept	(1×10^{-5})	(2×10^{-5})	(9×10^{-6})
	Earthquake Magnitude	1.7106	1.6098	1.8113
$\mathbf{A_{18}}$	Intercept	(6×10^{-8})	(9×10^{-8})	(4×10^{-8})
	Earthquake Magnitude	2.2792	2.1401	2.4184
$\mathbf{A_{34}}$	Intercept	(3×10^{-8})	(5×10^{-8})	(1×10^{-8})
	Earthquake Magnitude	2.1127	1.9266	2.2987

Table 4. A table of estimated coefficients for the best-fit statistical model shown in Figure 5. The upper and lower 95% confidence intervals for each fitted model is shown. This data is shown plotted in Figure 5.

Model	**Covariate**	**Estimated coefficient**	**95% Confidence Interval**	
			Lower limit	**Upper limit**
Earthquake	Intercept	0.028	0.0198	0.0396
	Earthquake Magnitude	0.9604	0.9184	1.0024
Earthquake-and-Landslide	Intercept	0.0797	0.0007	8.9187
	Earthquake Magnitude	1.0591	1.2645	0.8536

Table 5. A table of the significant covariates (at the 95% confidence level) associated with fatalities determined by backward stepwise multiple regression analysis. Covariates are shown in order of significance and with their associated statistics. The upper and lower limit at the 95% confidence interval for each covariate is also shown.

Covariate	**Estimated Parameter**	**Estimated Standard Error**	***t*-value**	**P(>|*t*|)**	**95% Confidence Interval**	
					Lower Limit	**Upper Limit**
Intercept	-1.806	6.137×10^{-1}	-2.944	0.00368	-3.009153	-6.036567×10^{-1}
PopExp18	2.123×10^{-7}	4.807×10^{-8}	4.415	1.75×10^{-5}	1.180359×10^{-7}	3.064799×10^{-7}
LS.NoLS	9.614×10^{-1}	2.310×10^{-1}	4.162	4.91×10^{-5}	5.085989×10^{-1}	1.414142
EQ.M	3.348×10^{-1}	8.148×10^{-1}	4.109	6.06×10^{-5}	1.750993×10^{-1}	4.944906×10^{-1}
BS	1.841×10^{-1}	7.028×10^{-2}	2.619	0.00957	4.633698×10^{-2}	3.218353×10^{-1}

Table 6. Predicted fatalities from earthquakes and earthquakes-and-landslides using the fatality model in Equation 6 when a M_w8 earthquake occurs for selected cities at risk from both earthquakes and landslides. The ranges of fatalities are calculated from the models 95% confidence intervals.

City	Country	Predicted Earthquake Fatalities (and 95% confidence interval estimates)	Predicted Earthquake-and-Landslide Fatalities (and 95% confidence interval estimates)
Permet	Albania	110 (1-323)	1002 (11-2958)
Rreshen	Albania	44 (0-129)	400 (4-1180)
Manizales	Colombia	4670 (53-13782)	42728 (479-126099)
Cartago	Costa Rica	352 (4-1038)	3217 (36-9494)
Alajuela	Costa Rica	8 (0-23)	70 (1-207)
Guaranda	Ecuador	604 (7-1783)	5529 (62-16317)
La Tacunga	Ecuador	204 (2-601)	1864 (21-5500)
San Miguel	El Salvador	43 (0-128)	397 (4-1172)
Sonsonate	El Salvador	196 (2-579)	1794 (20-5295)
Antigua	Guatemala	45 (1-134)	415 (5-1226)
Solola	Guatemala	44 (0-131)	406 (5-1197)
Yuscaran	Honduras	101 (1-298)	922 (10-2711)
Nagasaki	Japan	387 (4-1141)	3537 (40-10437)
Haka	Myanmar	111 (1-327)	1013 (11-2989)
New Plymouth	New Zealand	8 (0-23)	72 (1-212)
Arawa	Papua New Guinea	8 (0-25)	77 (1-229)
Mendi	Papua New Guinea	83 (1-246)	762 (9-2249)
Abancay	Peru	86 (2-255)	790 (9-2333)
Nal'chik	Russia	112 (1-329)	1021 (11-3013)
Bitlis	Turkey	97 (1-286)	886 (10-2616)
Coruh	Turkey	55 (1-164)	507 (6-1497)
Merida	Venezuela	164 (2-483)	1496 (17-4416)

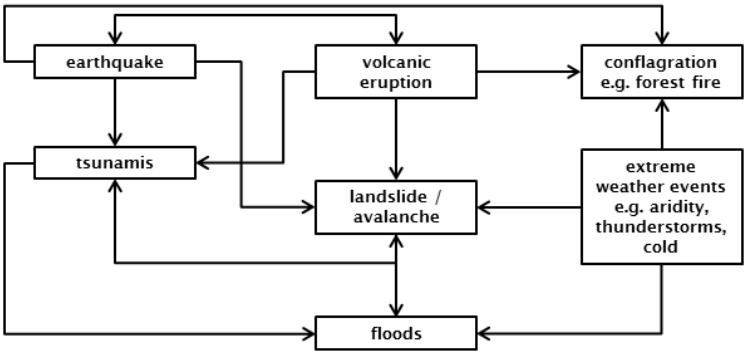

Fig. 1. The interconnected network of one hazard affecting another. Adapted from Helbing et al. (2005, p14).

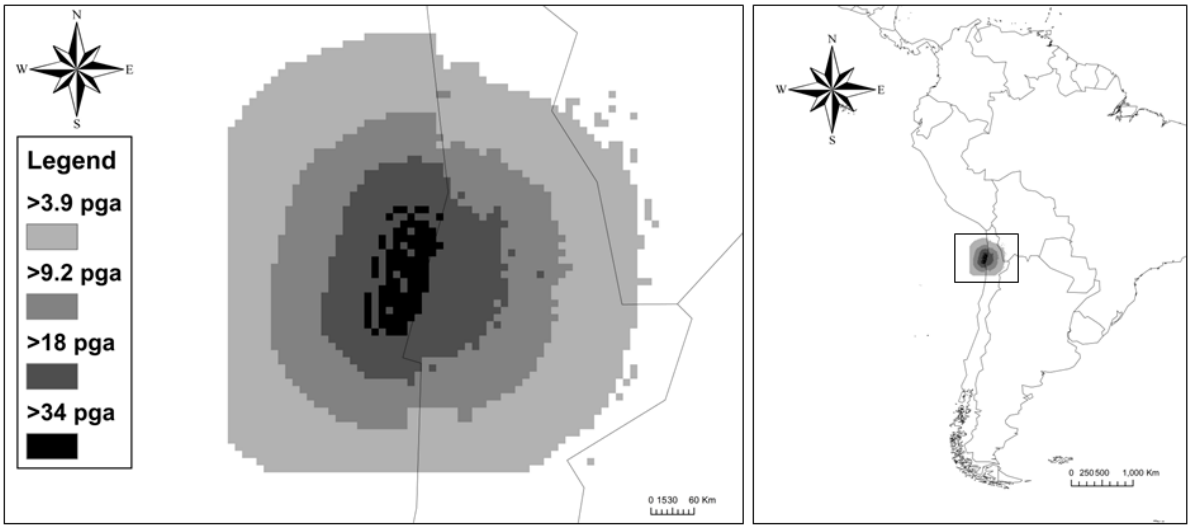

Fig. 2. Example of a peak ground acceleration ShakeMap from the USGS archive representing the Chilean earthquake on 15th November 2007. Cell colours on a grey scale represent peak ground acceleration (%g) for thresholds of ⩾3.9 pga, ⩾9.2 pga, ⩾18 pga, and ⩾34 pga shaking. The area affected by each level of shaking was calculated for 28 events between 2004 and 2009 from the USGS ShakeMap archive. The data were ussed to create models to predict area affected by different levels of shaking given recorded earthquake moment magnitude at the epicentre.

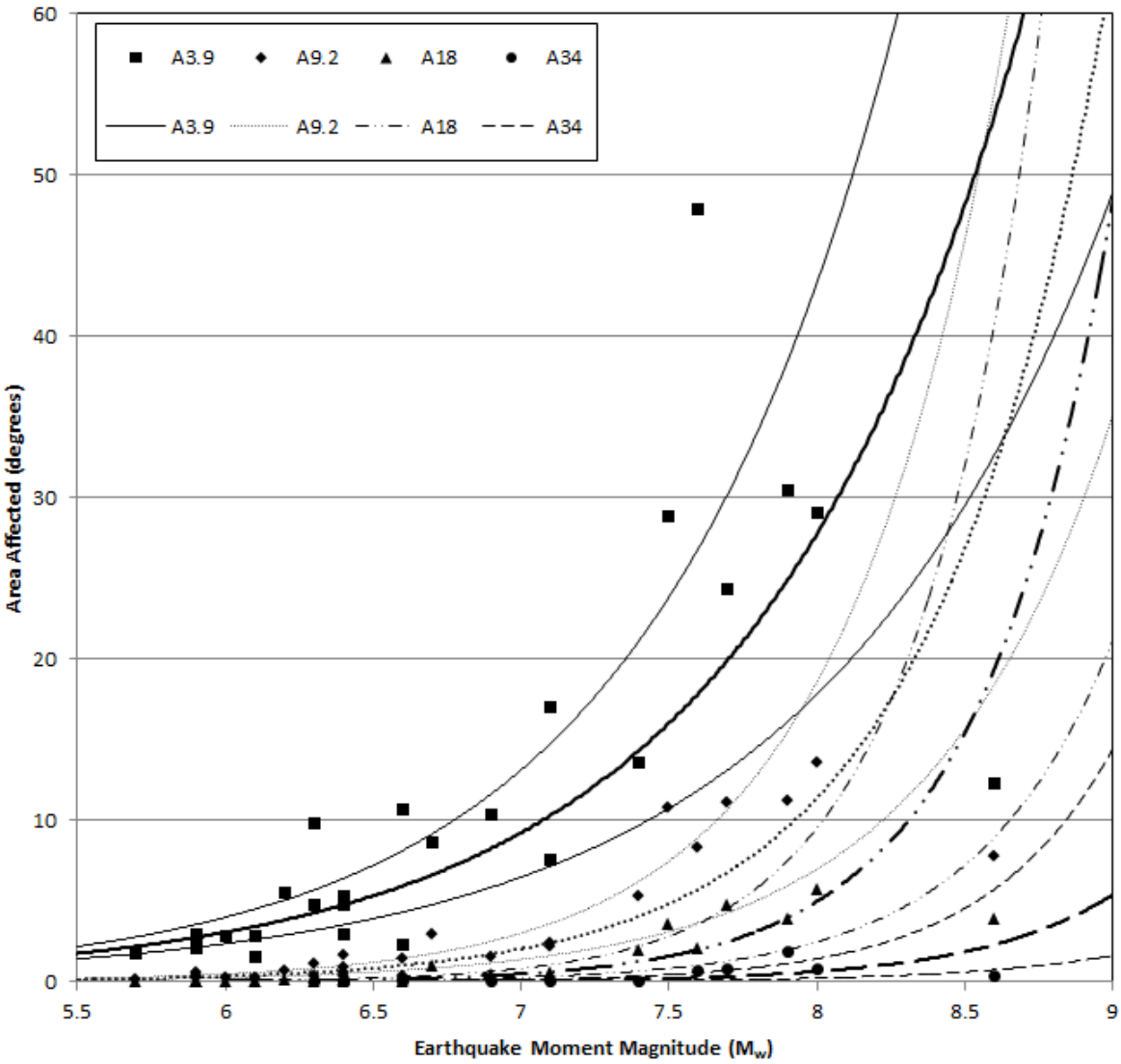

Fig. 3. Area affected (degrees) for different levels of shaking (⩾3.9 pga, ⩾9.2 pga, ⩾18 pga, and ⩾34 pga) and models fitted to the data based on earthquake moment magnitude (M_w). The area affected by each level of shaking was estimated from 28 events between 2004 and 2009 from the USGS ShakeMap archive. The models were used to estimate population exposed to shaking to be used in the multiple regression analysis. Each model's 95% confidence limit is plotted using the same type of line as the best-fit model. The best-fit regression is shown in bold.

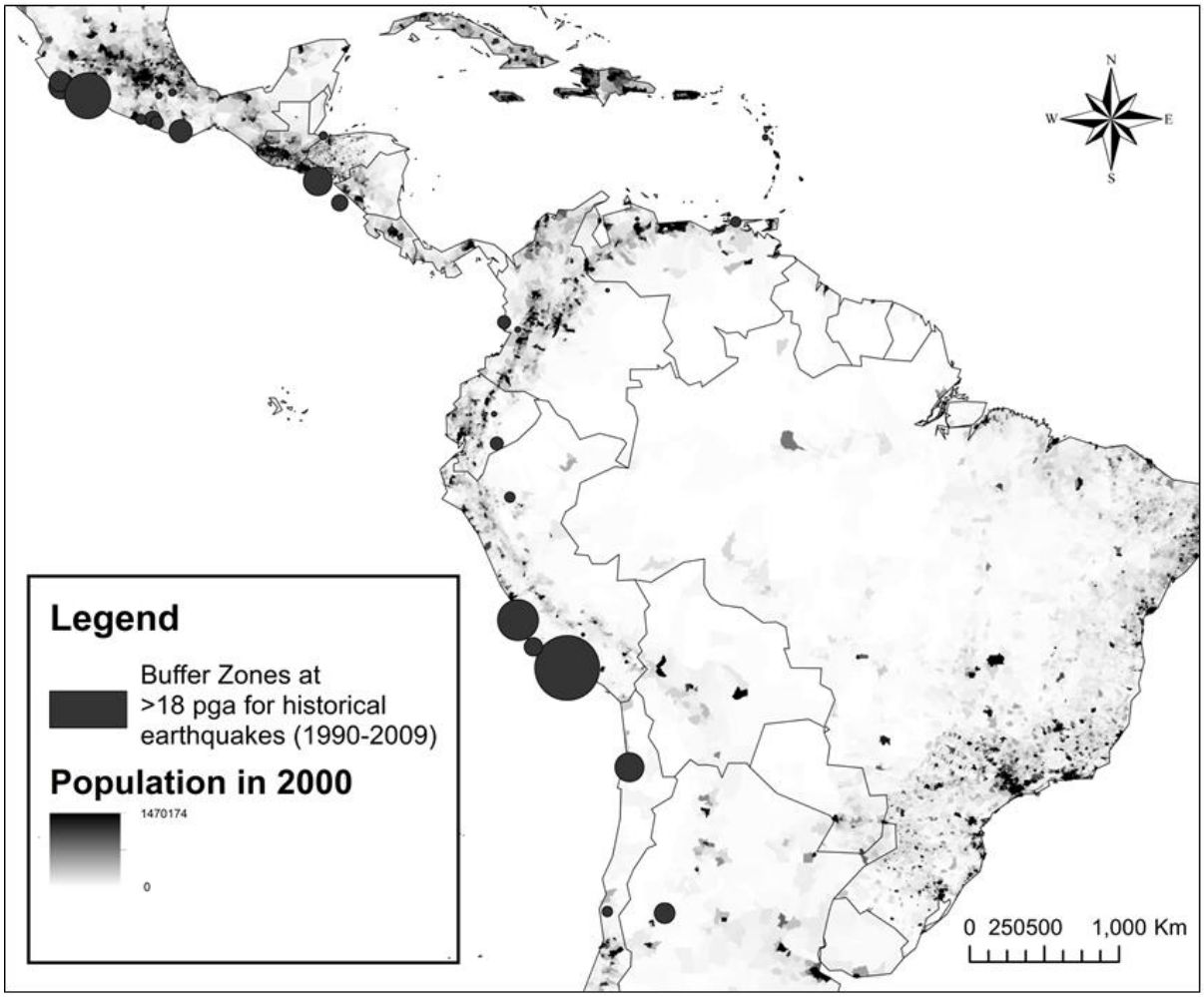

Fig. 4. An example of buffer zones around historical earthquakes in Central and South America in the PAGER-CAT database causing one or more fatalities (1990-2009) using radius of area for ≥18 pga. The buffer zones were determined from the models for area affected for different levels of shaking (⩾3.9 pga, ⩾9.2 pga, ⩾18 pga, and ⩾34 pga) based on recorded epicentre moment magnitude data. Gridded Population of the World for 2000 data are also shown. The population data were used to count the number of people living within each buffer zone, providing the estimated population exposed to different levels of shaking, to be used in the multiple regression model.

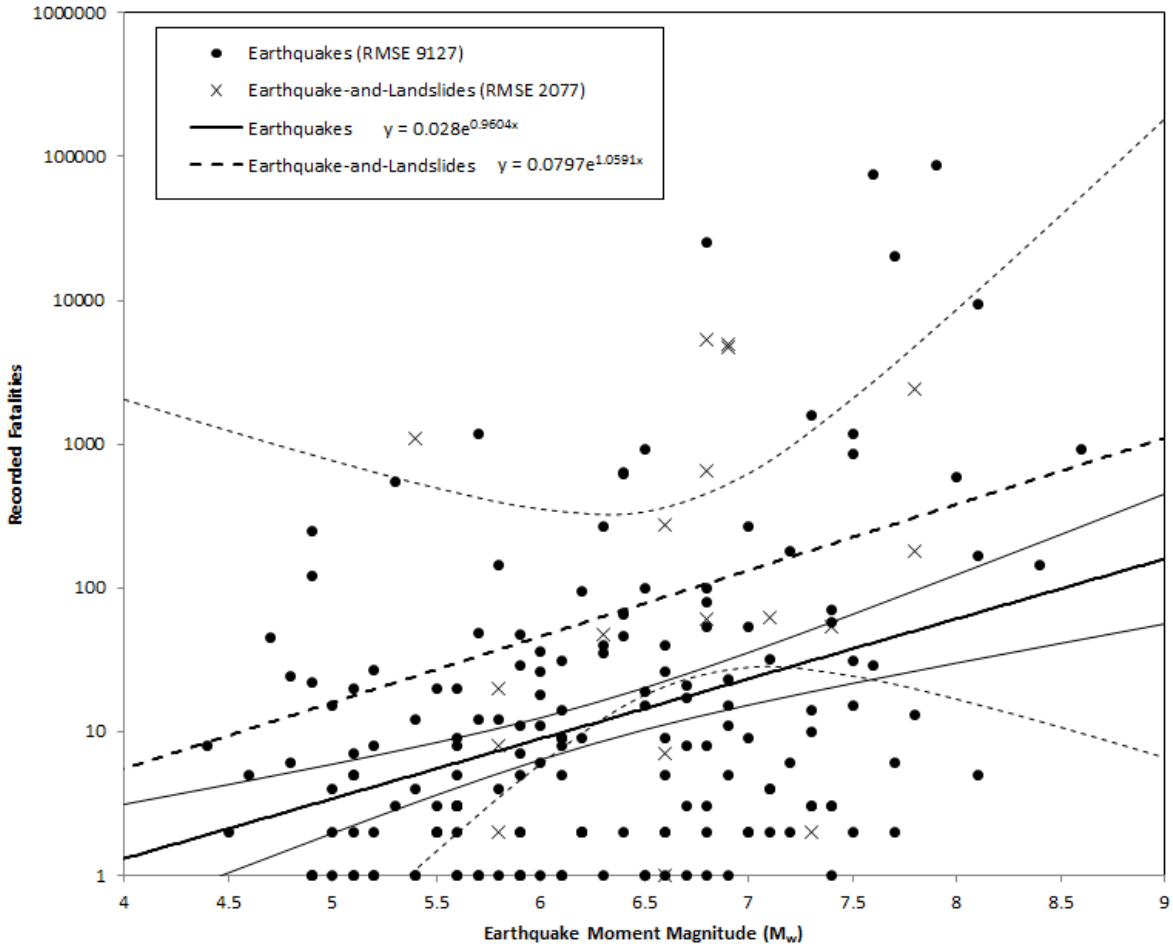

Fig. 5. Log of the number of recorded historical fatalities with respect to moment magnitude for 172 earthquakes and 18 earthquake-and-landslides with fitted exponential models. Data were sourced from PAGER-CAT, EM-DAT and Rodriguez et al. (1999) datasets described in section *2.0 Data*. The best-fit regression for Earthquake and Earthquake-and-Landslide models are shown in bold. Each model's 95% confidence limit is plotted using the same type of line as the best-fit model.

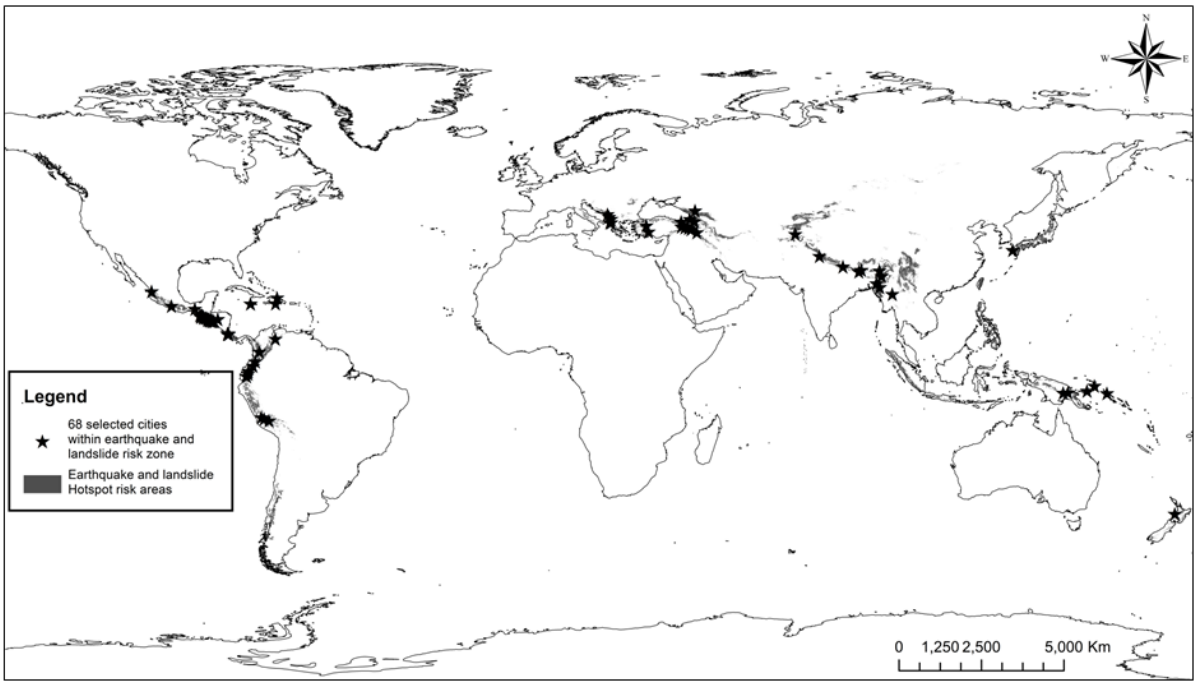

Fig. 6. Areas at risk from both earthquakes and landslides. A map was produced from the overlap of the Global Distribution of Earthquake Risk of Mortality and Global Distribution of Landslide Risk of Mortality maps produced in the Hotspots report (Dilley et al. 2005). Starred points indicate the location of 68 cities within this at risk area which were used as the epicentres for simulated earthquakes. The number of fatalities estimated by the model for simulated earthquakes and earthquake-and-landslide events were recorded and are shown in Figure 7.

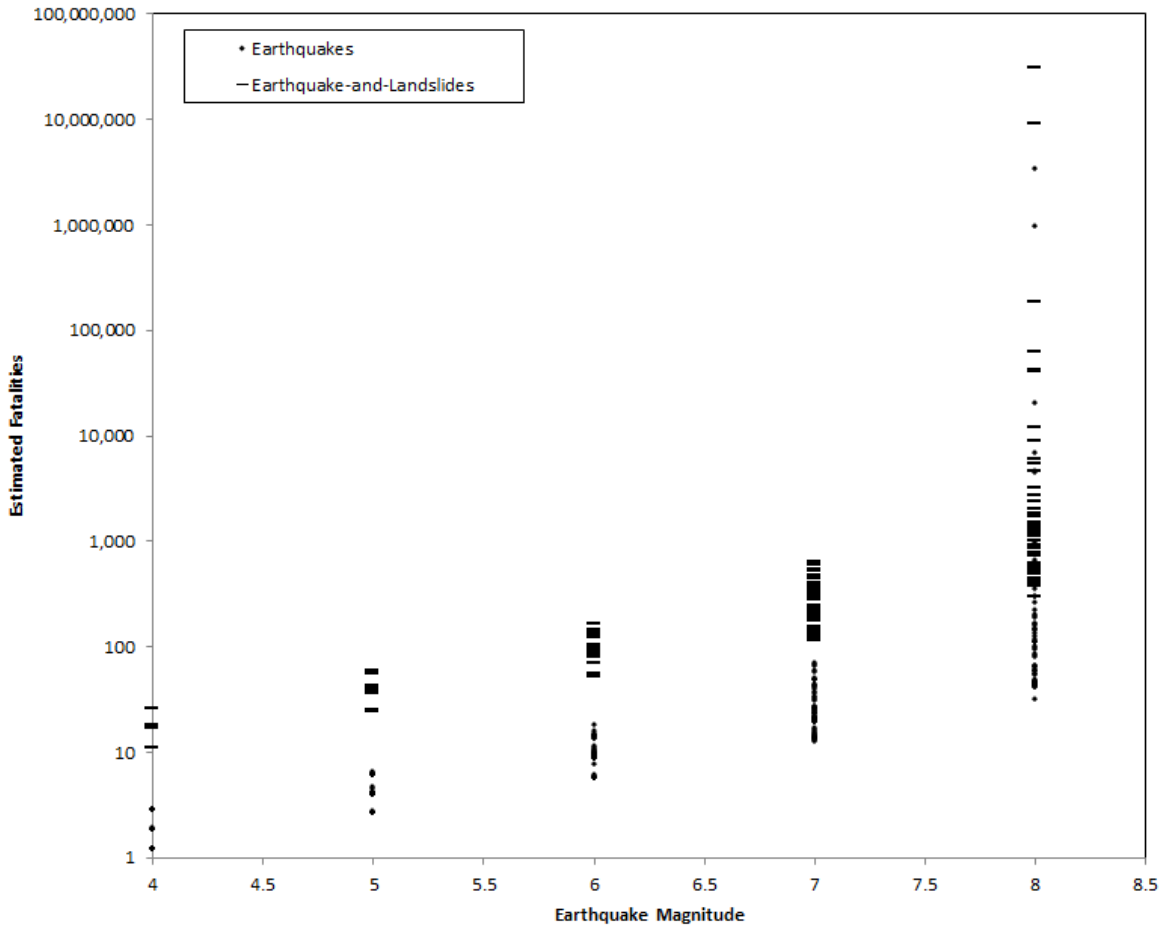

Fig. 7. Plot of estimated number of fatalities for 68 cities given an earthquake at the city centre for magnitudes of M_w 4, 5, 6, 7 and 8. Fatalities were estimated for earthquake-only and earthquakes- and-landslide scenarios.